

Kinetics of the early development of uniparental human haploid embryos

María-José Escribá, Ph.D.,^a Laura Escrich, Ph.D.,^a Yolanda Galiana, Ph.D.,^a Noelia Grau, Ph.D.,^a Arancha Galán, Ph.D.,^a and Antonio Pellicer, M.D.^{b,c}

^a IVF Laboratory and ^b Department of Reproductive Medicine, Instituto Valenciano de Infertilidad (IVI Valencia), University of Valencia; and ^c Reproductive Medicine Research Group, Instituto de Investigación Sanitaria La Fe, La Fe University Hospital, Valencia, Spain

Objective: To describe morphokinetically the early development of human haploid parthenotes and androgenotes and to compare them with euploid embryos.

Design: Experimental study of kinetics.

Setting: University-affiliated private fertility center.

Patient(s): Experimental haploid parthenotes and androgenotes.

Intervention(s): Kinetic study of early development (up to eight cells) of 8 parthenotes, 10 androgenotes, and 20 euploid embryos.

Main Outcome Measure(s): Timing of the first seven cleavages determined according to embryo origin, then calculation of the duration of the second and third cell cycles (cc2 and cc3) of whole embryos and individual cells.

Result(s): Parthenotes and androgenotes were experimentally produced by artificial oocyte activation and intracytoplasmic sperm injection of enucleated oocytes, respectively. Uniparental embryos having 6 to 10 cells were assessed for haploidy, their kinetics analyzed, retrospectively compared with euploid embryos. All the first seven cleavages occurred later in parthenotes than in both androgenotes and correctly fertilized embryos. The whole embryos and single cells showed that cc2 was longer in parthenotes than in both androgenotes and correctly fertilized embryos; cc3 was shorter in androgenotes than in both parthenotes and correctly fertilized embryos. The duration of cc2 versus cc3 was longer in correctly fertilized embryos and parthenotes than in androgenotes.

Conclusion(s): Parthenotes and androgenotes have different kinetics. The former have a longer cc2, and the latter a consistently shorter cc3 in comparison with correctly fertilized embryos. (Fertil Steril® 2016;105:1360–8. ©2016 by American Society for Reproductive Medicine.)

Key Words: Androgenote, haploid, human, morphokinetic, parthenote

Discuss: You can discuss this article with its authors and with other ASRM members at <http://fertstertforum.com/escribamj-kinetics-uniparental-haploid-embryos/>



Use your smartphone to scan this QR code and connect to the discussion forum for this article now.*

* Download a free QR code scanner by searching for "QR scanner" in your smartphone's app store or app marketplace.

Uniparental (parthenogenetic and androgenetic) embryos, each with their unique set of maternal and paternal chromosomes, constitute a useful model for investigating the existence of developmental differences according to haploidy and parental origin of human embryos. Most previous studies of uniparental embryo development have employed diploid or diploidized parthenogenetic (or gynogenetic) and androgenetic embryos. Few have assessed purely and

entirely hemizygous haploid uniparental embryos, which might represent the most feasible approximation to study unilaterally the constituents of the embryo.

Parthenogenesis involves artificial oocyte activation (AOA), which can be achieved by a wide range of physical and chemical stimuli that mimic the Ca^{2+} oscillations induced by the sperm during natural fertilization. Although human oocytes are successfully activated by such stimuli, the majority of

parthenotes arrest early in their development (1–6). Nevertheless, a few studies have reported successful parthenogenetic blastocyst formation (7–12). Such contrasting reports with respect to the development of parthenotes might be due to varying oocyte quality, the effectiveness of the AOA protocol applied, or more probably the ploidy of the parthenotes, as reported in other mammalian species (13–19). After AOA based on ionomycin incubation alone (1, 4, 5, 20, 21) or in combination with a protein synthesis inhibitor such as puromycin (6, 20, 22–27), most oocytes (60% to 75%) extrude the second polar body and form a single pronuclear structure with a DNA content that is compatible with a haploid set of chromosomes (4, 20, 21, 24, 26). However, a detailed description of

Received August 1, 2015; revised December 18, 2015; accepted December 28, 2015; published online January 22, 2016.

M.-J.E. has nothing to disclose. L.E. has nothing to disclose. Y.G. has nothing to disclose. N.G. has nothing to disclose. A.G. has nothing to disclose. A.P. has nothing to disclose.

Supported by the Instituto Pequeña y Mediana Industria Valenciana (IMPIVA: IMIDTF/2009/142; IMIDTF/2010/82, Generalitat Valenciana) and IVI Valencia.

Reprint requests: María-José Escribá, Ph.D., Instituto Universitario IVI, Instituto Valenciano de Infertilidad, Plaza Policia Local, 3, Valencia 46015, Spain (E-mail: mariajose.escriba@ivi.es).

in vitro development under these circumstances has not been provided to date, probably due to the difficulty in obtaining parthenotes beyond the four-cell (2, 6) or eight-cell (1, 4, 7) stage.

On the other hand, the developmental capacity of haploid androgenotes, produced by in vitro fertilization of enucleated metaphase 2 (MII) oocytes (19,28–30) or removal of the female pronucleus from the zygote (30–32), has been studied extensively in mice (28,33–39) and, to a lesser extent, in bovine (19), ovine (32), and porcine (40) species and in humans (30). Most of the studies in question have assessed the development of diploid androgenetic (diploidized monospermic or bispermic) embryos, but few have focused on that of haploid androgenotes [mice (28, 33, 34), bovine (19), human (30)].

Regardless of differences related to species and the methodology used to produce haploid androgenotes, the evidence to date confirms the poor capacity of these embryos for development. Research shows that most mouse haploid androgenotes cleave successfully but their development is arrested after the first few divisions, with only a few developing into blastocysts (28, 33, 34). That said, Kono et al. (28) reported that 60% and 11% of haploid androgenotes developed into eight-cell embryos and blastocysts, respectively. In another study, nearly 3% of bovine haploid androgenotes were found to progress to the compact morula stage, but only 1.8% developed into blastocysts (19). More limited developmental rates have been reported in humans (30); in the study in question, the percentage of androgenotes reaching the two- to eight-cell stage ranged from 65% to 90%, depending on the methodology used to produce them. Unfortunately, no further details were provided regarding their development.

In our present study, we describe for the first time the kinetic development of haploid human parthenotes and androgenotes from the one- to eight-cell stage using time-lapse monitoring. Moreover, by comparing retrospectively these embryos with correctly fertilized (biparental) embryos that become healthy babies (euploid embryos), we have determined how development differs according to haploidy and parental origin.

MATERIALS AND METHODS

This research was conducted at the Instituto Universitario IVI Valencia. All procedures and protocols for androgenote and parthenote production were approved by the institutional review board (0703-E-404-ME and 073-E-402-ME, respectively) and by the Spanish government (National Committee for Assisted Human Reproduction).

Oocyte Origin for Uniparental Embryo Production

For uniparental androgenote and parthenote production, MII oocytes were retrieved from healthy donors (aged between 18 and 35 years old) by follicular puncture and aspiration after a standard ovarian stimulation protocol. After cumulus removal, 60 mature oocytes were cryopreserved by vitrification according to the Cryotop method previously described by Kuwayama et al. (41), with slight modifications (42). In brief, oocytes were equilibrated in 7.5% (v/v) ethylene glycol

and 7.5% (v/v) dimethyl sulfoxide in TCM199 medium with 20% synthetic serum substitute at room temperature for 15 minutes. They were then placed in the vitrification solution containing 15% ethylene glycol, 15% dimethyl sulfoxide, and 0.5 M sucrose. After 1 minute in this solution, oocytes were placed on the Cryotop strip and immediately plunged into sterile liquid nitrogen (Ceralyn Online; Air Liquid France). Cryopreserved oocytes were stored pending signed informed consent to use them for the current research purposes.

For warming, each Cryotop was removed from the liquid nitrogen and placed in 1.0 M sucrose in TCM199 20% synthetic serum substitute at 37°C. After 1 minute, the oocytes were placed in 0.5 M sucrose in TCM199 20% synthetic serum substitute at room temperature for 3 minutes. Finally, the oocytes were washed for 6 minutes in TCM199 20% synthetic serum substitute at room temperature before they were incubated in cleavage medium for 2 hours (42). The oocytes were assessed for survival, and those with a healthy cytoplasm appearance without signs of atresia or degeneration (91.7% vitrification survival rate) were used for haploid androgenote and parthenote production.

Haploid Parthenogenote Production

For parthenote production, 25 surviving warmed MII oocytes were artificially activated using a calcium ionophore (A23187) and puromycin incubation (24, 26, 27). In short, the oocytes were exposed for 5 minutes to A23187 (4 mM; Sigma-Aldrich) and were subsequently cultured for 5 hours in puromycin (10 µg/mL; Sigma-Aldrich). After the AOA protocol had been applied, the eggs were cultured in a time lapse-system in 25 µL of cleavage medium. After 16 to 20 hours of culture, the eggs were assessed for extrusion of the second polar body and number of pronuclei. Although several types of oocyte activation response have been reported (15–17, 26, 43), only parthenotes that had extruded the second polar body and had a single maternal pronucleus (n = 13; 52.0% of haploid parthenotes) were subsequently cultured in a time-lapse system for 3 additional days, as described herein.

Haploid Androgenote Production

Androgenote production was performed according to the procedure described by Kono et al. (28, 29), with some modifications. In short, the procedure involves enucleation of MII oocytes and subsequent intracytoplasmic sperm injection (ICSI).

For MII oocyte enucleation, 30 surviving, warmed oocytes were inspected for the presence of the meiotic spindle using a light microscope equipped with Octax PolarAid (Olympus) imaging software. Once detected, the spindle was removed by gentle aspiration through an ICSI pipette (Cook) according to the procedure described by Grau et al. (44). One hour later, absence of the spindle was confirmed in the 21 oocytes that had survived manipulation (70.0% successful enucleation rate). Ooplasts were then microinjected following the conventional ICSI procedure and cultured in an Embryo-Slide (Unisense Fertilitech) containing 25 µL of cleavage medium with 1.2 mL of overlay of mineral oil (Cook). After this

process, they were cultured in a time-lapse system (EmbryoScope; Unisense Fertilitech).

After 16 to 20 hours of culture, time-lapse images were examined to identify the androgenotes that contained a single pronucleus (the paternal) and no second polar body in the perivitelline space ($n = 16$; 76.2% fertilization rate). These unipronucleated eggs were subsequently cultured for 3 additional days, as described herein.

Biparental Correctly Fertilized Embryos

To compare the morphokinetic data relating to the early development of the haploid parthenotes and androgenotes with the kinetics of heteroparental diploid (euploid) embryos, we investigated our clinical database for [1] coetaneous reproductive cycles in infertile couples without male infertility, [2] who had enrolled in our oocyte donation program and [3] received cryopreserved donated oocytes, and [4] whose embryos were cultured in a time-lapse incubator for 3 days and [5] were chromosomally analyzed in association to our implantation genetic screening program. Unfortunately, there were no clinical cases that agreed with these criteria, particularly with reference to the chromosomal analysis of the embryos. In consequence, we opted for 20 retrospectively selected embryos produced by ICSI of vitrified/warmed oocytes that had been obtained as part of our oocyte donation program; they were correctly fertilized (two polar bodies and two pronuclei) and subsequently were cultured in a time-lapsed incubator. Moreover, such day-3 embryos, after being intrauterinely transferred to the corresponding synchronized recipients ($n = 14$) over the course of this research did finally become into healthy live babies. Morphokinetic data relating to the early development of the correctly fertilized, euploid embryos were retrospectively collected.

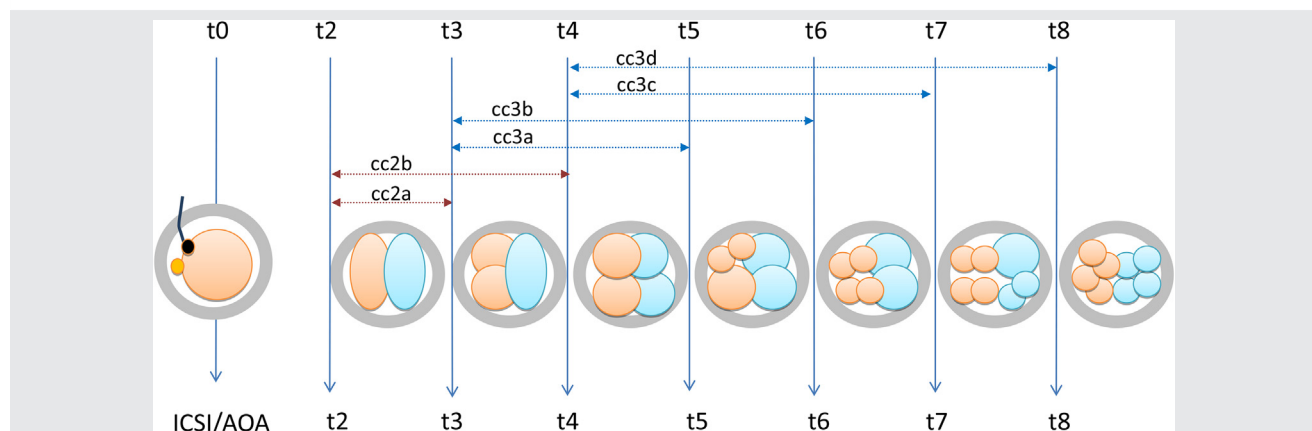
Embryo Culture

Immediately after ICSI (androgenotes and correctly fertilized embryos) or AOA (parthenotes), the eggs were placed in the EmbryoSlides and cultured for 3 days in the EmbryoScope. The EmbryoScope is an incubator with a built-in camera that records individual digital images at preprogrammed time intervals (e.g., every 15–20 minutes) while the embryos are maintained in constant culture conditions (5.5% CO_2 , 21% atmospheric O_2 , and 37.4°C). Images were captured by a monochromatic Leica camera with 1,280 \times 1,024 pixels, at a magnification of $\times 200$.

The direct kinetic variables of the parthenotes, androgenotes and correctly fertilized embryos were retrospectively obtained from time-lapse recordings acquired using the Embryo Viewer software (Unisense Fertilitech), which revealed development to the eight-cell stage of the androgenotes and parthenotes that were assessed for haploidy. Similarly, morphokinetic data of correctly fertilized embryos were obtained; specifically, the precise timing of the following developmental events was registered in terms of hours after ICSI or AOA (reference time; t_0): cleavage to the two-cell (t_2), three-cell (t_3), four-cell (t_4), five-cell (t_5), six-cell (t_6), seven-cell (t_7), and eight-cell (t_8) stages. Time of cleavage was defined as the moment in which cell division (cytokinesis) was completed.

Having determined the embryo cleavage timings from the two- to eight-cell stages, the following indirect variables (stated in hours) were calculated from the previously reported direct variables (Fig. 1): duration of the second cell cycle of the first blastomere to cleave from the two- to the three-cell stages ($\text{cc2a} = t_3 - t_2$); duration of the second cell cycle of the second blastomere to cleave from the two- to the four-cell stages ($\text{cc2b} = t_4 - t_2$); duration of the third cell cycle of the first ($\text{cc3a} = t_5 - t_3$), second ($\text{cc3b} = t_6 - t_4$), third ($\text{cc3c} = t_7 - t_4$), and fourth ($\text{cc3d} = t_8 - t_4$) blastomeres to cleave to the five-, six-, seven-, and eight-cell stages, respectively.

FIGURE 1



Embryo developmental events (model A) showing direct and indirect kinetic variables. The time reference (t_0) is with respect to artificial oocyte activation (AOA) in parthenotes or ICSI in androgenotes and correctly fertilized embryos. The direct kinetic variables were as follows: time of embryo cleavage to the two-, three-, four-, five-, six-, seven-, and eight-cell stages ($t_2, t_3, t_4, t_5, t_6, t_7, t_8$). The indirect kinetic variables were as follows: duration of the second cell cycle of the first blastomere to cleave from the two- to the three-cell stage ($\text{cc2a} = t_3 - t_2$); duration of the second cell cycle of the second blastomere to cleave from the two- to the four-cell stage ($\text{cc2b} = t_4 - t_2$); duration of the third cell cycle of the first ($\text{cc3a} = t_5 - t_3$), second ($\text{cc3b} = t_6 - t_4$), third ($\text{cc3c} = t_7 - t_4$), and fourth ($\text{cc3d} = t_8 - t_4$) blastomeres to cleave to the five-, six-, seven-, and eight-cell stages, respectively.

Escribá. Kinetics in uniparental haploid embryos. *Fertil Steril* 2016.

of cc2a and cc2b; and duration of the third cell cycle of the first (cc3a), second (cc3b), third (cc3c), and fourth (cc3d) blastomeres to cleave to the five-, six-, seven-, and eight-cell stages, respectively. Tracking the blastomere origin was necessary to determine cc3a, cc3b, cc3c, and cc3d, as it has been recently described (45). When an embryo displayed cleavage pattern A, B, or C, the cc3a was obtained by calculating $t_5 - t_3$, whereas if an embryo cleaved according to pattern D, E, or F, the cc3a was defined as $t_5 - t_4$. Similarly, cc3b was obtained by calculating $t_6 - t_3$ (according to model A, D, or E) or $t_6 - t_4$ (according to model B, C, or F). The cc3c duration was calculated as $t_7 - t_4$ (according to model A, C, or E) or $t_7 - t_3$ (according to model B, D, or F), whereas cc3d was obtained by calculating $t_8 - t_4$ (according to model A, B, or D) or $t_8 - t_3$ (according to model C, E, or F). The cc3 values of cc3a-d allowed us to calculate an average cc3, where $acc3 = (cc3a + cc3b + cc3c + cc3d)/4$.

The degree of blastomere cleavage synchrony (referred to as synchrony degree, or SD) was also calculated in the second (SD2) and third (SD3) cell cycles. The SD2 was defined as cc2a/cc2b and ranged from 0 to 1. The SD3 was calculated by $[(cc3a + cc3b + cc3c + cc3d)/4]/(t_8 - t_3)$, and also ranged from 0 to 1.

Chromosome Analysis

For chromosome determination, parthenotes and androgenotes of more than six cells were selected for biopsy following the methodology routinely used at IVI Valencia for preimplantation genetic diagnosis or screening (46). In short, parthenotes and androgenotes were placed in a droplet containing Ca^{2+} - and Mg^{2+} - free medium (G-PGD; Vitrolife), and the zona pellucida was perforated using laser technology (OCTAX). All blastomeres were individually removed by aspiration using a biopsy pipette with an inner diameter of 30 μm (Humagen). After the embryo biopsy, individual blastomeres were incubated in a hypotonic solution and then transferred onto a grease-free slide to spread and lyse the cells. The chromosomal analysis was performed by means of fluorescence in situ hybridization (FISH) for five chromosomes (X, Y, 13, 18, and 21) using CEPX (Spectrum Blue), CEPY (Spectrum Gold), LSI13 (Spectrum Orange), CEP18 (Spectrum Aqua), and LSI21 (Spectrum Green). Samples were analyzed with an Olympus AX-70 epifluorescence microscope (Olympus Optical), and the images were recorded with an Olympus DP-50 camera.

Statistical Analyses

The in vitro development of the embryos of different origins was compared using the chi-square test, and Yates's correction for continuity was applied when appropriate. Similar statistical tests were performed to compare the frequency distribution of the embryo cleavage patterns according to the origin of the embryo.

For each continuous variable, the normality of the samples was confirmed using the Kolmogorov-Smirnov test. Because the data of the continuous variables were adjusted to normal distributions, direct and indirect variables were analyzed using the analysis of variance test. Data were

presented as mean \pm standard deviation with the 95% confidence interval (95% CI), when appropriate. When a multiple comparison was performed, Bonferroni's correction was applied. $P \leq .05$ was considered statistically significant. All statistical analyses were performed using the Statistical Package for the Social Sciences 19.0 (IBM).

RESULTS

Uniparental In Vitro Development

With respect to early in vitro development, 13 (81.2%) of 16 androgenotes and all 13 parthenotes (100%) cleaved. In relation to subsequent in vitro development, the eight-cell stage was reached by 10 (62.5%) of 16 androgenotes and 8 (61.5%) of 13 parthenotes. No statistically significant differences in early in vitro development were observed between parthenotes and androgenotes, so we can affirm that 89.6% of uniparental embryos cleaved and 62.1% progressed to the eight-cell stage. In the case of the group of correctly fertilized embryos, all 20 embryos cleaved and progressed to the eight-cell stage, as expected.

The haploidy of uniparental embryos was confirmed in all androgenotes (23,X0 and 23,Y0, according to the 4:6 ratio) and parthenotes (23,X0). Therefore, morphokinetic studies were performed of 10 androgenotes, 8 parthenotes, and all 20 correctly fertilized embryos, which yielded a total of 20 healthy babies. In this sense, although fewer in number, the uniparental embryos formed a uniform and consistent experimental group. In fact, the analysis of the data distribution (performed by Kolmogorov-Smirnov) confirmed the normality of the samples with respect to all the continuous variables analyzed. Accordingly, statistical analyses of direct and indirect kinetic variables were performed using the analysis of variance test or comparison test for independent samples when appropriate.

Direct Variables Analysis

The first cell cycle terminates when the embryo cleaves into two cells (t_2). Our recordings indicated that this event and subsequent cleavages up to the eight-cell stage (from t_2 to t_8) occurred statistically significantly later in parthenotes than in both androgenotes and correctly fertilized embryos (Table 1).

Indirect Variables Analysis

To accurately calculate the indirect variables, the embryo cleavage pattern was determined by cell-tracking analysis, which revealed that the distribution of cleavage patterns did not differ statistically according to embryo origin. In brief, all 8 parthenotes, 9 of 10 androgenotes, and 15 of 20 correctly fertilized embryos followed the A-C models of cleavage (100%, 90%, and 75%; $P > .05$). Surprisingly, one androgenote followed model F, 4 of the 20 correctly fertilized embryos (20%) displayed a cleavage pattern compatible with model D, and 1 of the correctly fertilized embryos (5%) followed model E.

Assessment of indirect kinetic variables (Table 2) revealed that the duration of the second cell cycle of both sister

TABLE 1**Direct variables of uniparental (parthenotes and androgenotes) and correctly fertilized embryos.**

Timing (h)	Parthenotes (n = 8)	Androgenotes (n = 10)	Correctly fertilized embryos (n = 20)
Cleavage to the stage of			
2-cell (t2)	30.6 ± 3.5 (26.3–34.9) ^a	24.9 ± 2.4 (22.9–27.0) ^b	25.4 ± 2.8 (24.1–26.7) ^b
3-cell (t3)	44.9 ± 4.5 (39.3–50.5) ^a	36.7 ± 3.4 (33.9–39.6) ^b	37.0 ± 3.6 (35.3–38.7) ^b
4-cell (t4)	46.3 ± 3.7 (41.7–50.8) ^a	37.4 ± 3.1 (34.9–40.0) ^b	37.5 ± 3.7 (35.7–39.2) ^b
5-cell (t5)	62.8 ± 6.0 (55.4–70.2) ^a	50.8 ± 6.3 (45.6–56.0) ^b	53.1 ± 5.8 (50.4–55.8) ^b
6-cell (t6)	63.9 ± 5.5 (57.0–70.8) ^a	53.2 ± 7.0 (47.4–59.1) ^b	54.1 ± 5.9 (51.3–56.8) ^b
7-cell (t7)	67.3 ± 7.5 (58.0–76.7) ^a	53.7 ± 6.6 (47.6–59.8) ^b	55.3 ± 5.9 (52.6–58.1) ^b
8-cell (t8)	70.9 ± 8.6 (49.5–92.4) ^a	51.6 ± 4.9 (43.8–59.4) ^b	58.1 ± 6.4 (55.1–61.2) ^b

Note: The direct variables were the timings (mean ± standard deviation) of embryo cleavages to the two (t2), three (t3), four (t4), five (t5), six (t6), seven (t7), and eight (t8) cell stages, referred to as hours after artificial oocyte activation (parthenotes) or intracytoplasmic sperm injection (androgenotes and correctly fertilized embryos). The values between brackets denote the 95% confidence interval for all the cleavage timings.

^{a,b} Different superscripts in the same row represent statistical differences (P ≤ .05).

Escribá. *Kinetics in uniparental haploid embryos. Fertil Steril* 2016.

blastomeres (cc2a and cc2b) was statistically comparable among parthenotes (average: 15.0 ± 1.8 hours), androgenotes (average: 12.1 ± 1.1 hours), and correctly fertilized embryos (average: 11.8 ± 1.2 hours). However, comparison of the second cell cycle according to embryo origin (see Table 2) showed that cc2a, cc2b, and, in consequence, the average mean duration of the second cell cycle (acc2) was statistically significantly longer in parthenotes than in both androgenotes and correctly fertilized embryos, with the latter two groups being statistically comparable. On the basis of this, the average cc2a (11.6 ± 1.2 hours; 95% CI, 11.2–12.1 hours), cc2b (12.2 ± 1.2 hours; 95% CI, 11.7–12.6 hours), and acc2 (11.9 ± 1.2 hours; 95% CI, 11.5–12.3 hours) were calculated.

At the four-cell stage, the duration of the third cell cycle was determined for each blastomere and was found to be statistically comparable within each uniparental group, which allowed us to calculate the average mean duration of cc3 (acc3) for parthenotes (20.4 ± 3.8 hours; 95% CI, 10.8–30.0 hours) and androgenotes (13.5 ± 2.0 hours; 95% CI, 10.3–16.7 hours). However, comparison of the acc3 among uniparental embryos showed statistically significant differences between parthenotes and androgenotes, with this phase

lasting longer in the former case (see Table 2). Concerning correctly fertilized embryos, we observed that duration of the third cell cycle of each blastomere was not uniform; the cell cycle duration was comparable among the first three blastomeres to cleave (average cc3a–c: 16.7 ± 2.8 hours; 95% CI, 16.0–17.5 hours) but was statistically significantly shorter than in the fourth blastomere to cleave (cc3d: 20.5 ± 4.4 hours) (see Table 2). In consequence, it was not considered appropriate to calculate the acc3.

Comparison of cc3a, cc3b, and cc3c according to embryo origin revealed that the duration of these phases was comparable among parthenotes, androgenotes, and correctly fertilized embryos (see Table 2). However, the cc3d was statistically significantly shorter in androgenotes than in both parthenotes and correctly fertilized embryos, in which the duration of this phase was statistically similar (average: 20.9 ± 4.4 hours; 95% CI, 19.0–22.7 hours).

Comparison of the duration of cc2 and cc3 in individual androgenetic blastomeres revealed similar values (average: 14.3 ± 4.0 hours; 95% CI, 13.0–15.5 hours). However, in the case of parthenogenetic cells, the cell cycle duration in the third and fourth blastomeres to cleave (cc3c and cc3d)

TABLE 2**Indirect variables of uniparental haploid human embryos (parthenotes and androgenotes) and correctly fertilized embryos.**

Indirect variables of	Parthenotes (n = 8)	Androgenotes (n = 10)	Correctly fertilized embryos (n = 20)	Average
cc2a	14.3 ± 1.6 (12.3–16.4) ^a	11.8 ± 1.2 (10.7–12.8) ^b	11.6 ± 1.1 (11.0–12.1) ^b	NA
cc2b	15.7 ± 2.1 (13.0–18.3) ^a	12.5 ± 1.0 (11.6–13.4) ^b	12.0 ± 1.2 (11.5–12.6) ^b	NA
acc2	15.0 ± 1.9 (13.6–16.4) ^a	12.1 ± 1.2 (11.5–12.8) ^b	11.8 ± 1.2 (11.4–12.2) ^b	NA
cc3a	17.8 ± 2.3 (14.9–20.7) ^b	14.0 ± 3.6 (11.0–17.0) ^b	15.8 ± 2.6 (14.6–17.0) ^b	15.6 ± 3.0 (14.6–16.7)
cc3b	18.6 ± 1.8 (16.4–20.8) ^b	16.0 ± 4.5 (12.2–19.7) ^b	16.8 ± 2.6 (15.6–18.0) ^b	16.8 ± 3.1 (15.8–17.9)
cc3c	21.4 ± 3.8 (16.7–26.2) ^b	17.4 ± 6.4 (11.5–23.2) ^b	17.7 ± 3.0 (16.3–19.1) ^b	18.2 ± 4.1 (16.7–19.7)
cc3d	22.5 ± 4.2 (15.9–29.1) ^b	14.5 ± 1.9 (11.5–17.5) ^b	20.5 ± 4.4 (18.4–22.6) ^b	NA
acc3	20.0 ± 3.4 (18.3–21.6) ^b	15.5 ± 4.5 (13.7–17.3) ^b	17.7 ± 3.6 (16.9–18.5) ^b	NA
SD2, at the 2-cell stage	0.92 ± 0.08 (0.82–1.00) ^b	0.94 ± 0.03 (0.91–0.97) ^b	0.96 ± 0.02 (0.95–0.97) ^b	0.95 ± 0.04 (0.94–0.96)
SD3, at the 4-cell stage	0.87 ± 0.007 (0.84–0.89) ^b	0.88 ± 0.06 (0.78–0.97) ^b	0.85 ± 0.09 (0.81–0.90) ^b	0.86 ± 0.08 (0.83–0.89)

Note: The indirect variables, presented as mean ± standard deviation (95% confidence interval) and referred to as hours, indicate: duration of the first and second blastomeres to cleave to the two-cell stage (cc2a and cc2b); duration of the third cell cycle in each blastomere (cc3a–cc3d) and average duration of the second (acc2) and third cell cycles (acc3). The blastomere synchrony between cleavage in the second (SD2) and third (SD3) cell cycle is also presented. The values between brackets denote the 95% confidence interval for all the variables.

^{a,b} Different superscript values in the same row indicate statistical significance (P ≤ .05). NA = not applicable; it was not feasible to provide the average mean of the variable because there were statistical differences between the uniparental and correctly fertilized embryos for the corresponding kinetic variable.

Escribá. *Kinetics in uniparental haploid embryos. Fertil Steril* 2016.

was statistically significant longer (average: 21.9 ± 3.8 hours; 95% CI, 19.0–24.8 hours) than acc2 (15.0 ± 1.8 hours; see Table 2), whereas that of the first and second blastomeres to cleave (cc3a and cc3b) had an intermediate duration with respect to acc2 and cc3 in their sister blastomeres (average: 18.2 ± 2.0 hours; 95% CI, 16.8–19.6 hours). The cell cycles of correctly fertilized blastomeres were longer in the three first blastomeres to cleave (cc3a-c) than in acc2 (16.7 ± 2.8 hours vs. 11.8 ± 1.2 hours, respectively), and were longest in the case of the fourth blastomeres to cleave (cc3d: 20.5 ± 4.4 hours; see Table 2).

When we compared the duration of cc2 versus cc3 in whole embryos according to their origin, we observed that the third cell cycle was significantly longer in correctly fertilized embryos (average: 5.9 ± 2.1 hours; 95% CI, 4.9–6.9 hours) and parthenotes (average: 5.5 ± 1.9 ; 95% CI, 2.4–8.6 hours), whereas the duration of both cell cycles was almost the same among androgenotes (average interval between acc2 and acc3: 2.1 ± 1.4 hours; 95% CI, 0.1–5.5 hours).

The degree of cleavage synchrony in the second (SD2) and third (SD3) cell cycles was high and comparable for all embryo origin (see Table 2). However, among androgenotes and correctly fertilized embryos, the degree of cleavage synchrony significantly dropped between the second and third cell cycle (average SD2: 0.96 ± 0.03 vs SD3: 0.85 ± 0.09), while it remained unaltered among parthenotes (average: 0.9 ± 0.07).

DISCUSSION

Ours is the first study to describe the kinetics of uniparental haploid human embryos over the course of their early in vitro development using time-lapse technology. Uniparental haploid embryos are capable of progressing through the early stages of in vitro development regardless of their maternal or paternal genomic composition.

Our results regarding the in vitro development of haploid parthenotes revealed that 61.5% progressed in vitro to the eight-cell stage. This contrasts with the findings of earlier reports concerning human parthenogenesis, in which almost all parthenotes were reported to cleave, many arrested at the four-cell stage, and only 10% to 20% progressed to the eight-cell stage (1, 2, 4, 6, 20). The greater developmental ability of our parthenotes may have been related to the applied AOA and/or to the oocyte quality because all the oocytes in question were obtained from donor women.

Results were also encouraging in the case of haploid androgenotes, with 62.5% progressing in vitro to the eight-cell stage. In vitro development of human and mice haploid androgenotes seems to be conditioned considerably by the procedure used to produce them (19, 28, 30, 34, 47). In this respect, two approaches have been proposed, based on the removal of the meiotic spindle from MII oocytes followed by in vitro fertilization or based on enucleation of fertilized telophase II oocytes/elimination of the female pronucleus from fertilized eggs (epronucleation). In humans, enucleation of telophase II oocytes is reported to be the most efficient technique for androgenote production (100%) (31); however, this strategy, and the removal of the female pronucleus from fertilized eggs, implies the destruction of a

recently constituted embryo, with its inherent ethical implications.

In the present work, we chose to produce androgenotes by fertilizing enucleated MII oocytes, and achieved a global technical efficiency estimated at 53.3% (70% successful enucleation and 76.2% fertilization rate), which is comparable to the efficacy reported by Kuznyetsov et al. (30), who used a similar approach (51.5%). Unfortunately, the investigators in question did not provide a detailed description of their androgenotes' development, merely indicating that 64.7% reached the two- to eight-cell stage. In our study, 62.5% of our androgenotes progressed to the eight-cell stage. Moreover, fluorescence in situ hybridization (FISH) studies confirmed that androgenotes at the eight-cell stage were haploid and accomplished the 2:3 sex ratio—that is, there were both Y- and X-bearing androgenotes. These results differ from those reported in mice (34, 48), in which it has been observed that Y-bearing haploid androgenotes do not develop beyond the first few cleavage divisions. Unfortunately, we cannot affirm whether human haploid androgenotes and parthenotes are capable of progressing to the blastocyst stage, or at what rate, because our androgenotes were not cultured beyond day 3 of development due to the lack of specific governmental permission for such a purpose.

Kinetic analysis of embryo cleavage using time-lapse monitoring revealed that all first seven cleavages took place later in parthenotes than in both androgenotes and correctly fertilized embryos. The delayed cleavages observed in parthenotes with respect to androgenotes and correctly fertilized embryos could be due to the associated activation procedure itself, because the spermatozoon, which we used to produce both androgenotes and normally fertilized embryos, is the activating agent par excellence; alternatively, the observed delayed cleavages may have been a consequence of the varying durations of the phases that make up the first cell cycle. However, we did not study this aspect, as time-lapsed culture of parthenotes began once the second polar body had been extruded (during 5-hour puromycin incubation, AOA), with pronuclear appearing being the first morphokinetic event to be registered. Nevertheless, because the reference time point for all the embryo origins studied here was AOA or ICSI, or more feasibly the timing for pronuclear fading (Supplemental Table 1, available online), discrepancies in cleavage timings are attributable to the particular nature or ploidy of the individual embryos, although the possible effect of the solutions or procedure used to generate parthenotes and androgenotes cannot be ruled out because neither a control solution nor sham-injected oocytes were included.

In any case, we thought it would be accurate to describe embryo kinetics according to the indirect variables, which provides us with a reliable morphokinetic description of embryo development independent of any reference time point: duration of the cell cycles of whole embryos and each single cell, and degree of blastomere cleavage synchrony. In this way, this is the first report that describes the kinetics of human haploid parthenogenetic and androgenetic development and compares them with those of correctly individually fertilized embryos, including those of the blastomeres that compose them.

The second cell cycle was similar in androgenotes and correctly fertilized embryos. Given that the correctly fertilized embryos developed into viable offspring, we assume that the values in question are optimal and represent normal development. The second cell cycle of androgenotes and correctly fertilized embryos was short in all cases (average: 11.9 ± 1.2 hours), probably because the gap phases (G1, G2) were short or absent. In parthenotes, on the other hand, the second cell cycle was longer than in the other two groups (average: 15.0 ± 1.9 hours). Because both parthenotes and androgenotes were uniparental haploid embryos, ploidy could not have been the origin of such discrepancies. Indeed, the absence of the sperm in parthenotes would be the most feasible explanation of the longer duration of the second cycle.

Besides triggering oocyte activation, the fertilizing spermatozoon endows the oocyte with the centriole and paternal chromatin. It is the most efficient activating agent, as it triggers oocyte activation naturally and is responsible for initiating the developmental program established in the ooplasm during oogenesis. In this sense, despite the efficiency of the AOA procedure in inducing an adequate initial activation of the oocyte (i.e., extrusion of the second polar body and pronuclear formation), it could have been responsible for the longer cell cycles and delayed cleavages observed in parthenotes. However, we have no data to affirm this.

The fertilizing spermatozoon also endows the oocyte with the centriole, an active division center. Although parthenotes do not possess such an extra-chromosome structure, they are capable of cleaving in its absence, probably due to the reactivation of remnants of the maternal microtubule organizing center or through the interlocking of maternal proteins that join with one another or with the remnants of a primordial template, which would allow a rudimentary bipolar mitotic spindle to be built at a slower rate (49, 50). The constitution of a functional mitotic center in parthenotes may require more time, which would contribute to a longer cell cycle.

The spermatozoon also provides the oocyte with the paternal chromatin, which differs from the maternal type in structure, nuclear positoning, transcriptional activity, and pattern of histone/DNA modifications. Indeed, the maternal and paternal pronuclei have been reported to display distinct patterns of DNA methylation reprogramming at fertilization in mice and humans, but not in sheep or rabbits. The zygotic paternal chromatin undergoes an active, rapid, and drastic DNA demethylation before the first DNA replication; while the maternal chromatin, though exposed to the same cytoplasm, is resistant to this active demethylation process and remains highly methylated (51–53). In consequence, the maternal methylation level remains constant throughout the first cell cycle but becomes passively demethylated by a semiconservative replication-dependent mechanism which initiated at the two-cell embryo stage. Whether DNA replication occurs more slowly in methylated versus unmethylated DNA, the pattern of DNA methylation in parthenotes would explain their longer second cycle, which contrasts with the shorter cycle observed in theoretically unmethylated androgenetic DNA. However, this does not explain the short second cycle observed in correctly fertilized embryos.

Recently, ultralarge-scale whole-transcriptome analysis in mice has revealed that the absence of paternally sperm-borne-derived molecules, including noncoding RNA and chromatin-associated proteins, alters the appropriate gene expression at the onset of minor gene activation, also known as zygotic genome activation. As a consequence, promiscuous gene expression might occur in parthenotes but not in androgenotes or correctly fertilized embryos, in which the presence of such paternally derived factors might suppress nascent RNA production (i.e., transcriptional repression) (54, 55). Thus, we hypothesize that whether or not human embryos display a regulatory activation program similar to that described in mice, the longer second cell cycle observed in our parthenotes could have been due to the gap phases (G1, G2) that stemmed from an altered gene expression which occurred concomitantly with the onset of zygotic genome activation, recently described to take place in human embryos as early as the two-cell stage (56).

Whether the absence of the centriole, differential parental DNA demethylation dynamics, the altered genome transcription in parthenotes, or all (or some) of these factors are the cause of the observed discrepancies in the duration of the second cell cycle among parthenotes and androgenetic and correctly fertilized embryos is unclear. Moreover, it is beyond the scope of this discussion because we did not analyze the specific phases of the first cell cycle or the methylation or the transcriptome profiles of each blastomere.

The third cell cycle in the whole embryo was persistently shorter in androgenotes (average: 15.5 ± 4.5 hours) than in parthenotes and correctly fertilized embryos (average: 18.1 ± 3.1 hours), which can be explained by the lack of female endowment. In correctly fertilized human embryos, the major onset of embryonic genome activation (EGA) generally occurs at the four- to eight-cell stage (56–58) or on day 3 of development or afterward (59, 60). Cinematographic analysis of pig embryo development has shown the cell cycle at the onset of the EGA to be longer than in pretranscriptional embryo stages (61, 62), as was also observed in cat (63) and bovine (64) embryos. Under our experimental conditions, the third cell cycle of correctly fertilized embryos lasted 17.7 ± 3.6 hours, while the second cycle lasted 11.8 ± 1.2 hours. Similarly, analyses of the duration of the cell cycles of individual blastomeres and the degree of cleavage synchrony between the two-cell cycles suggested that blastomeres of correctly fertilized embryos changed from a homogeneous to a heterogeneous population between the second and third cell cycles. Similarly, analysis of the duration of the second and the third cell cycles of whole embryos and of each blastomere of our haploid parthenotes revealed a moderate lengthening between these two consecutive cell cycles.

The molecular reason for this slowing down of embryo development and the heterogeneity of blastomeres in association with the onset of genome transcription may have been due to the gap phases that appear autonomously for each blastomere, as recently suggested by Wong et al. (58). The investigators used single-cell gene expression analysis to demonstrate that some of the blastomeres of a single

eight-cell embryo maintained maternal mRNAs, whereas others progressed to the EGA.

In addition, we cannot rule out the implication of maternal chromatin methylation, which, after successive rounds of semiconservative DNA replication, would have reached a low methylation level at the eight-cell stage (51), with only one blastomere conserving the original methylated patterning. In this context, haploid parthenotes and correctly fertilized embryos would display the major EGA during the third cell cycle, when both parental chromatins are completely demethylated in almost all blastomeres of an embryo.

Conversely, in androgenotes, the sustained short cell cycle duration and high degree of cleavage synchrony throughout the second and third cycles (average: 14.3 ± 4.0 hours; 95% CI, 13.0–15.5 hours) leads us to believe that our haploid androgenotes were made up of a homogeneous cell population during these two consecutive cell cycles and that the major EGA does not occur in haploid androgenotes during the same developmental stages as it does in correctly fertilized embryos. Therefore, early androgenetic development might progress under a reduced or absent transcriptional activity thanks to the maintenance of maternal and paternal mRNAs, which have been detected in correctly fertilized human embryos up until day 3 of development (58). This feature may be feasible due to either a low consumption of ooplasmic maternal proteins and messengers or the continued synthesis of some proteins of maternal origin [as has been observed in rat (65) and bovine (64, 66) embryos cultured in the presence of transcriptional inhibitors], or both. These observations encourage us to undertake future research into the androgenetic embryo transcriptome with the aim of determining whether androgenetic genome transcription exists, and, if not, to clarify the mechanism(s) by which such uniparental embryos progress in their early in vitro development.

In conclusion, throughout our morphokinetic analysis, we have noted differences and similarities between haploid uniparental and correctly fertilized embryos. In particular, the duration of the second and third cell cycle would seem to be defined by the parental composition (parthenote or androgenote) rather than by ploidy. This might be related to the precise and sequential regulation of the waves of transcriptional activation orchestrated by the maternal and paternal (epi)genome. Our pioneering study provides some clues for further research on human embryo development and endorses the use of haploid androgenotes and parthenotes as models with which to study parent-specific genetic and epigenetic reprogramming and transcription during the preimplantation development of human embryos. There is still a lack of knowledge about these aspects owing to the scarcity of human embryos for research and the ethical and legal aspects surrounding their use, obstacles that do not apply to haploid uniparental embryos.

Acknowledgments: The authors thank all the IVI staff, especially the embryologists; and B. Normanly for editing this manuscript.

REFERENCES

1. Winston N, Johnson M, Pickering S, Braude P. Parthenogenetic activation and development of fresh and aged human oocytes. *Fertil Steril* 1991;56: 904–12.
2. De Sutter P, Dozortsev D, Cieslak J, Wolf G, Verlinsky Y, Dyban A. Parthenogenetic activation of human oocytes by puromycin. *J Assist Reprod Genet* 1992;9:328–37.
3. De Sutter P, Dozortsev D, Vrijens P, Desmet R, Dhont M. Cytogenetic analysis of human oocytes parthenogenetically activated by puromycin. *J Assist Reprod Genet* 1994;11:382–8.
4. Taylor AS, Braude PR. The early development and DNA content of activated human oocytes and parthenogenetic human embryos. *Hum Reprod* 1994;9: 2389–97.
5. Rinaudo P, Pepperell JR, Buradgunta S, Massobrio M, Keefe DL. Dissociation between intracellular calcium elevation and development of human oocytes treated with calcium ionophore. *Fertil Steril* 1997;68:1086–92.
6. Nakagawa K, Yamano S, Moride N, Yamashita M, Yoshizawa M, Aono T. Effect of activation with Ca ionophore A23187 and puromycin on the development of human oocytes that failed to fertilize after intracytoplasmic sperm injection. *Fertil Steril* 2001;76:148–52.
7. Lin H, Lei J, Wininger D, Nguyen MT, Khanna R, Hartmann C, et al. Multilineage potential of homozygous stem cells derived from metaphase II oocytes. *Stem Cells* 2003;21:152–61.
8. Mai Q, Yu Y, Li T, Wang L, Chen MJ, Huang SZ, et al. Derivation of human embryonic stem cell lines from parthenogenetic blastocysts. *Cell Res* 2007; 17:1008–19.
9. Paffoni A, Brevini TA, Somigliana E, Restelli L, Gandolfi F, Ragni G. In vitro development of human oocytes after parthenogenetic activation or intracytoplasmic sperm injection. *Fertil Steril* 2007;87:77–82.
10. Revazova ES, Turovets NA, Kochetkova OD, Kindarova LB, Kuzmichev LN, Janus JD, et al. Patient-specific stem cell lines derived from human parthenogenetic blastocysts. *Cloning Stem Cells* 2007;9:432–49.
11. de Fried EP, Ross P, Zang G, Divita A, Cunniff K, Denadai F, et al. Human parthenogenetic blastocysts derived from noninseminated cryopreserved human oocytes. *Fertil Steril* 2008;89:943–7.
12. Versieren K, Heindryckx B, Lierman S, Gerris J, De Sutter P. Developmental competence of parthenogenetic mouse and human embryos after chemical or electrical activation. *Reprod Biomed Online* 2010;21:769–75.
13. Henery CC, Kaufman MH. Cleavage rate of haploid and diploid parthenogenetic mouse embryos during the preimplantation period. *Mol Reprod Dev* 1992;31:258–63.
14. Kim NH, Uhm SJ, Ju JY, Lee HT, Chung KS. Blastocoele formation and cell allocation to the inner cell mass and trophectoderm in haploid and diploid pig parthenotes developing in vitro. *Zygote* 1997;5:365–70.
15. Escriba MJ, Garcia-Ximenez F. Electroactivation of rabbit oocytes in an hypotonic pulsing medium and parthenogenetic in vitro development without cytochalasin B-diploidizing pretreatment. *Theriogenology* 1999; 51:963–73.
16. Escriba MJ, Garcia-Ximenez F. Influence of sequence duration and number of electrical pulses upon rabbit oocyte activation and parthenogenetic in vitro development. *Anim Reprod Sci* 2000;59:99–107.
17. Escriba MJ, Garcia-Ximenez F. Use of a variable electrical pulsing sequence in rabbit oocyte activation. *Reprod Nutr Dev* 2000;40:261–9.
18. Latham KE, Akutsu H, Patel B, Yanagimachi R. Comparison of gene expression during preimplantation development between diploid and haploid mouse embryos. *Biol Reprod* 2002;67:386–92.
19. Lagutina I, Lazzari G, Duchi R, Galli C. Developmental potential of bovine androgenetic and parthenogenetic embryos: a comparative study. *Biol Reprod* 2004;70:400–5.
20. Rhoton-Vlasak A, Lu PY, Barud KM, Dewald GW, Hammitt DG. Efficacy of calcium ionophore A23187 oocyte activation for generating parthenotes for human embryo research. *J Assist Reprod Genet* 1996;13: 793–6.
21. Paffoni A, Paracchini V, Ferrari S, Scarduelli C, Seia M, Coviello DA, et al. Use of parthenogenetic activation of human oocytes as an experimental model for evaluation of polar body based PGD assay performance. *J Assist Reprod Genet* 2011;28:461–70.

22. Johnson MH, Pickering SJ, Braude PR, Vincent C, Cant A, Currie J. Acid Tyrode's solution can stimulate parthenogenetic activation of human and mouse oocytes. *Fertil Steril* 1990;53:266–70.

23. Yamano S, Nakagawa K, Nakasaka H, Aono T. Fertilization failure and oocyte activation. *J Med Invest* 2000;47:1–8.

24. Nakagawa K, Yamano S, Nakasaka H, Hinokio K, Yoshizawa M, Aono T. A combination of calcium ionophore and puromycin effectively produces human parthenogenotes with one haploid pronucleus. *Zygote* 2001;9:83–8.

25. Sengoku K, Takuma N, Miyamoto T, Yamauchi T, Ishikawa M. Nuclear dynamics of parthenogenesis of human oocytes: effect of oocyte aging in vitro. *Gynecol Obstet Invest* 2004;58:155–9.

26. Escrich L, Grau N, Mercader A, Rubio C, Pellicer A, Escriba MJ. Spontaneous in vitro maturation and artificial activation of human germinal vesicle oocytes recovered from stimulated cycles. *J Assist Reprod Genet* 2011;28:111–7.

27. Escrich L, Grau N, de los Santos MJ, Romero JL, Pellicer A, Escriba MJ. The dynamics of in vitro maturation of germinal vesicle oocytes. *Fertil Steril* 2012;98:1147–51.

28. Kono T, Sotomaru Y, Sato Y, Nakahara T. Development of androgenetic mouse embryos produced by in vitro fertilization of enucleated oocytes. *Mol Reprod Dev* 1993;34:43–6.

29. Kono T, Carroll J, Swann K, Whittingham DG. Nuclei from fertilized mouse embryos have calcium-releasing activity. *Development* 1995;121:1123–8.

30. Kuznyetsov V, Kuznyetsova I, Chmura M, Verlinsky Y. Duplication of the sperm genome by human androgenetic embryo production: towards testing the paternal genome prior to fertilization. *Reprod Biomed Online* 2007;14:504–14.

31. Barra J, Renard JP. Diploid mouse embryos constructed at the late 2-cell stage from haploid parthenotes and androgenotes can develop to term. *Development* 1988;102:773–9.

32. Hagemann LJ, Peterson AJ, Weilert LL, Lee RS, Tervit HR. In vitro and early in vivo development of sheep gynogenotes and putative androgenotes. *Mol Reprod Dev* 1998;50:154–62.

33. McGrath J, Solter D. Completion of mouse embryogenesis requires both the maternal and paternal genomes. *Cell* 1984;37:179–83.

34. Surani MA, Barton SC, Norris ML. Nuclear transplantation in the mouse: heritable differences between parental genomes after activation of the embryonic genome. *Cell* 1986;45:127–36.

35. Latham KE, Solter D. Effect of egg composition on the developmental capacity of androgenetic mouse embryos. *Development* 1991;113:561–8.

36. Mann JR, Stewart CL. Development to term of mouse androgenetic aggregation chimeras. *Development* 1991;113:1325–33.

37. Hagemann LJ, First NL. Embryonic cytoplasmic extracts rescue murine androgenes to the blastocyst stage. *Development* 1992;114:997–1001.

38. Latham KE, Sapienza C. Localization of genes encoding egg modifiers of paternal genome function to mouse chromosomes one and two. *Development* 1998;125:929–35.

39. Obata Y, Ono Y, Akuzawa H, Kwon OY, Yoshizawa M, Kono T. Post-implantation development of mouse androgenetic embryos produced by in-vitro fertilization of enucleated oocytes. *Hum Reprod* 2000;15:874–80.

40. Sembon S, Iwamoto M, Hashimoto M, Oishi T, Fuchimoto D, Suzuki S, et al. Porcine androgenetic embryos develop to fetal stage in recipient mothers. *Theriogenology* 2012;78:225–31.

41. Kuwayama M. Highly efficient vitrification for cryopreservation of human oocytes and embryos: the Cryotop method. *Theriogenology* 2007;67:73–80.

42. Cobo A, Kuwayama M, Perez S, Ruiz A, Pellicer A, Remohi J. Comparison of concomitant outcome achieved with fresh and cryopreserved donor oocytes vitrified by the Cryotop method. *Fertil Steril* 2008;89:1657–64.

43. Kaufman MH. The experimental production of mammalian parthenogenetic embryos. 1978;21–47.

44. Grau N, Escrich L, Albert C, Delgado A, De los Santos M, Escribá M. Comparison of two methodologies of oocyte enucleation. *Fertil Steril* 2011;96:S246.

45. Grau N, Escrich L, Galiana Y, Meseguer M, García-Herrero S, Remohí J, et al. Morphokinetics as a predictor of self-correction to diploidy in triplopronucleated intracytoplasmic sperm injection-derived human embryos. *Fertil Steril* 2015;104:728–35.

46. Rubio C, Rodrigo L, Mercader A, Mateu E, Buendia P, Pehlivan T, et al. Impact of chromosomal abnormalities on preimplantation embryo development. *Prenat Diagn* 2007;27:748–56.

47. Kono T, Kwon OY, Watanabe T, Nakahara T. Development of mouse enucleated oocytes receiving a nucleus from different stages of the second cell cycle. *J Reprod Fertil* 1992;94:481–7.

48. Morris T. The X0 and Oy chromosome constitutions in the mouse. *Genet Res* 1968;12:125–37.

49. Schatten G, Simerly C, Schatten H. Maternal inheritance of centrosomes in mammals? Studies on parthenogenesis and polyspermy in mice. *Proc Natl Acad Sci USA* 1991;88:6785–9.

50. Palermo GD, Colombero LT, Rosenwaks Z. The human sperm centrosome is responsible for normal syngamy and early embryonic development. *Rev Reprod* 1997;2:19–27.

51. Mayer W, Niveleau A, Walter J, Fundele R, Haaf T. Demethylation of the zygotic paternal genome. *Nature* 2000;403:501–2.

52. Barton SC, Arney KL, Shi W, Niveleau A, Fundele R, Surani MA, et al. Genome-wide methylation patterns in normal and uniparental early mouse embryos. *Hum Mol Genet* 2001;10:2983–7.

53. Beaujean N, Taylor JE, McGarry M, Gardner JO, Wilmut I, Loi P, et al. The effect of interspecific oocytes on demethylation of sperm DNA. *Proc Natl Acad Sci USA* 2004;101:7636–40.

54. Bui HT, Wakayama S, Mizutani E, Park KK, Kim JH, Van Thuan N, et al. Essential role of paternal chromatin in the regulation of transcriptional activity during mouse preimplantation development. *Reproduction* 2011;141:67–77.

55. Park SJ, Komata M, Inoue F, Yamada K, Nakai K, Ohsugi M, et al. Inferring the choreography of parental genomes during fertilization from ultralarge-scale whole-transcriptome analysis. *Genes Dev* 2013;27:2736–48.

56. Vassena R, Boue S, Gonzalez-Roca E, Aran B, Auer H, Veiga A, et al. Waves of early transcriptional activation and pluripotency program initiation during human preimplantation development. *Development* 2011;138:3699–709.

57. Braude P, Bolton V, Moore S. Human gene expression first occurs between the four- and eight-cell stages of preimplantation development. *Nature* 1988;332:459–61.

58. Wong CC, Loewke KE, Bossert NL, Behr B, De Jonge CJ, Baer TM, et al. Non-invasive imaging of human embryos before embryonic genome activation predicts development to the blastocyst stage. *Nat Biotechnol* 2010;28:1115–21.

59. Dobson AT, Raja R, Abeyta MJ, Taylor T, Shen S, Haqq C, et al. The unique transcriptome through day 3 of human preimplantation development. *Hum Mol Genet* 2004;13:1461–70.

60. Assou S, Boumela I, Haouzi D, Anahory T, Dechaud H, De Vos J, et al. Dynamic changes in gene expression during human early embryo development: from fundamental aspects to clinical applications. *Hum Reprod Update* 2011;17:272–90.

61. Anderson JE, Matteri RL, Abeydeera LR, Day BN, Prather RS. Cyclin B1 transcript quantitation over the maternal to zygotic transition in both in vivo- and in vitro-derived 4-cell porcine embryos. *Biol Reprod* 1999;61:1460–7.

62. Schoenbeck RA, Peters MS, Rickards LF, Stumpf TT, Prather RS. Characterization of deoxyribonucleic acid synthesis and the transition from maternal to embryonic control in the 4-cell porcine embryo. *Biol Reprod* 1992;47:1118–25.

63. Hoffert KA, Anderson GB, Wildt DE, Roth TL. Transition from maternal to embryonic control of development in IVM/IVF domestic cat embryos. *Mol Reprod Dev* 1997;48:208–15.

64. Lequarre AS, Marchandise J, Moreau B, Massip A, Donnay I. Cell cycle duration at the time of maternal zygotic transition for in vitro produced bovine embryos: effect of oxygen tension and transcription inhibition. *Biol Reprod* 2003;69:1707–13.

65. Zernicka-Goetz M. Activation of embryonic genes during preimplantation rat development. *Mol Reprod Dev* 1994;38:30–5.

66. Liu Z, Foote RH. Development of bovine embryos in KSOM with added superoxide dismutase and taurine and with five and twenty percent O2. *Biol Reprod* 1995;53:786–90.

SUPPLEMENTAL TABLE 1

Direct variables of uniparental (parthenotes and androgenotes) and correctly fertilized embryos.

Timing (h) t0 = PNF	Parthenotes (n = 8)	Androgenotes (n = 10)	Correctly fertilized embryos (n = 20)
Cleavage to the stage of			
2-cell (t2)	2.8 ± 0.7 (1.9–3.6) ^a	2.6 ± 0.5 (2.3–3.0) ^a	2.6 ± 0.5 (2.3–2.9) ^a
3-cell (t3)	17.1 ± 2.1 (14.5–19.7) ^b	14.4 ± 1.6 (13.1–15.7) ^a	14.0 ± 1.1 (13.5–14.6) ^a
4-cell (t4)	18.4 ± 2.2 (15.7–21.2) ^b	15.2 ± 1.3 (14.1–16.3) ^a	14.5 ± 1.1 (13.9–15.0) ^a
5-cell (t5)	35.0 ± 4.1 (30.0–40.0) ^b	28.5 ± 4.9 (24.4–32.6) ^a	29.8 ± 3.2 (28.3–31.4) ^a
6-cell (t6)	36.1 ± 3.3 (32.0–40.2) ^b	31.0 ± 5.6 (26.3–35.6) ^a	30.8 ± 3.3 (29.2–33.4) ^a
7-cell (t7)	39.5 ± 5.9 (32.2–46.8) ^b	31.6 ± 6.0 (26.1–37.2) ^a	32.1 ± 3.5 (30.4–33.8) ^a
8-cell (t8)	41.5 ± 6.7 (25.0–58.0) ^b	29.6 ± 2.5 (25.5–33.6) ^a	34.8 ± 4.6 (32.6–37.0) ^a

Note: The direct variables were the timings (mean ± standard deviation) of embryo cleavages to the two (t2), three (t3), four (t4), five (t5), six (t6), seven (t7) and eight (t8) cell stages, referred to as hours after pronuclear fading (PNF). The values between brackets denote the 95% confidence interval for all the cleavage timings.

^{a,b}Different superscripts in the same row represent statistical differences ($P \leq .05$).

Escribà. Kinetics in uniparental haploid embryos. *Fertil Steril* 2016.